A novel hybrid time-varying graph neural network for traffic flow forecasting

Ben-Ao Dai, Bao-Lin Ye

Abstract—Real-time and accurate traffic flow prediction is the foundation for ensuring the efficient operation of intelligent transportation systems. In existing traffic flow prediction methods based on graph neural networks (GNNs), pre-defined graphs were usually used to describe the spatial correlations of different traffic nodes in urban road networks. However, the ability of predefined graphs used to describe spatial correlation was limited by prior knowledge and graph generation methods. Although time-varying graphs based on data-driven learning can partially overcome the drawbacks of pre-defined graphs, the learning ability of existing adaptive graphs was limited. For example, time-varying graphs cannot adequately capture the inherent spatial correlations in traffic flow data. In order to solve these problems, we have proposed a hybrid time-varying graph neural network (HTVGNN) for traffic flow prediction. Firstly, a novel time-aware multi-attention mechanism based on time-varying mask enhancement was reported to more accurately model the temporal dependencies among distinct traffic nodes in the traffic network. Secondly, we have proposed a novel graph learning strategy to concurrently learn both static and dynamic spatial associations between different traffic nodes in road networks. Meanwhile, in order to enhance the learning ability of timevarying graphs, a coupled graph learning mechanism was designed to couple the graphs learned at each time step. Finally, the effectiveness of the proposed method HTVGNN was demonstrated with four real data sets. Simulation results illustrate that, compared with the latest space-time graph neural network model, the proposed method HTVGNN has higher prediction accuracy. In addition, the ablation experiment verifies that the coupled graph learning mechanism can effectively improve the long-term prediction performance of HTVGNN. The source code is located at: https://github.com/xxxxxx/HTVGNN.

Index Terms—unmanned vehicle, model predictive control, trajectory tracking.

I. Introduction

OWADAYS, with the acceleration of the urbanization process, the car ownership has increased sharply. Subsequently, how to improve the traffic efficiency of the road network to alleviate traffic congestion has always been a difficult problem [1]. Since it can provide the traffic state information for a certain period of time in the future based on real-time monitored traffic data, traffic flow prediction has been widely applied to improve the level of intelligent traffic management and control in road networks. In the early studies, researchers

This work was supported in part by Zhejiang Provincial Natural Science Foundation of China under Grant No.LTGS23F030002; and by the Jiaxing Public Welfare Research Program No.2023AY11034; and by the National Natural Science Foundation of China under Grant No. 61603154.

Ben-Ao Dai and Bao-Lin Ye are with the School of Information Science and Engineering, Jiaxing University, Jiaxing, Zhejiang, 314001, China; and also with the School of Information Science and Engineering, Zhejiang Sci-tech University, Xiasha Campus, Hangzhou, Zhejiang, 310018, China (email:yebaolin@zjxu.edu.cn, Daiba1201@163.com).

Corresponding author: Bao-Lin Ye (yebaolin@zjxu.edu.cn)

mainly used mathematical statistics based methods to construct traffic flow prediction models. For example, historical average (HA) [2] [3], autoregressive moving average model (ARIMA) [4] [5], vector autoregressive model (VAR) [6], etc. These statistics based methods assume that the dependency of timeseries data is linear. However, since traffic flow often has complex and changeable characteristics, the dependency of the traffic flow time-series data is nonlinear. As a result, the performance of statistics based methods is not well in actual traffic flow prediction tasks. After that, traditional machine learningbased methods (e.g. support vector regression (SVR) [7] and k-nearest neighbor (KNN) [8]) were reported to overcome the drawbacks of statistics based methods. Nevertheless, the performance of traditional machine learning-based methods mainly relies on the handcrafted features, which makes it difficult for them to fully utilize the increasingly abundant large-scale traffic flow data. Then, with the rapid development of deep learning, long short-term memory (LSTM) and their variants gated recurrent units (GRU) [9] were used to model the temporal dependencies of traffic flow time-series data, while convolutional neural networks (CNN) [10] and graph convolutional networks (GCN) [11] [12] [13] were employed to capture the spatial dependencies of different traffic nodes.

The first challenge lies in capturing the spatial correlation between roads more effectively, without relying on prior knowledge. Previous studies have predominantly relied on certain prior knowledge (such as distance, DTW, Pearson coefficient) to construct a spatial structure map that signifies the spatial relationship of road networks. Examples include Spatiotemporal Graph Convolution (STGCN) [14] and Spatiotemporal Fusion Graph Neural Network (STFGNN) [15], which calculate node correlations based on road distances and historical traffic data to establish a predefined spatial structure map between roads. However, these predefined maps often fail to accurately represent the traffic flow data and our prediction model. The expressiveness of such predefined maps depends heavily on the rationality of prior knowledge and graph generation methods employed, resulting in potential inclusion of unreasonable or incorrect spatial correlations that limit their effectiveness. To address this issue, Graph WaveNet (Graph WaveNet) has achieved some success by utilizing predetermined graphs for both forward and backward diffusion while incorporating adaptive graphs. Nevertheless, GWN still heavily relies on predetermined graphs for capturing spatial correlation. Adaptive Graph Convolutional Recurrent Network (AGCRN) [16] and Structure-aware Convolutional Neural Networks (SACNNs) [17] have further improved adaptive spatial modeling by achieving similar effects as predefined graph structures without any reliance on predetermined graphs at all. However, current adaptive graph learning typically involves learning a global adaptive graph for all time steps, thereby limiting its learning capability.

Furthermore, regardless of whether it is an adaptive or predefined graph, the spatial correlation described by it remains constant. However, the traffic network exhibits complexity and variability, with its topology undergoing intricate changes over time. Effectively modeling the dynamic spatial correlation between roads is therefore crucial in spatial correlation modeling.

In this paper, we propose a novel time-aware multi-head attention mechanism based on time-varying mask enhancement to address the aforementioned issues. The aim is to enhance the computational accuracy and time-awareness capability of multi-head attention.we focus on capturing the spatio-temporal characteristics of complex changes by introducing an efficient coupled time-varying graph convolutional recurrent network. This network utilizes time-varying graphs at each time step to learn the spatial dependencies within the road network. to improve its effectiveness in learning long-term dependencies, we integrate the learned time-varying graphs from different time steps. This approach enhances prediction performance by considering short-term traffic patterns between adjacent time steps. additionally, for effectively modeling dynamic spatial correlation within the road network, we propose a dynamic time-varying graph convolution that combines topology matrix and similarity matrix as a mask matrix for more effective modeling of dynamic spatial correlations.

The following are the four key contributions of our work in traffic flow prediction:

- A novel time-aware multi-head attention mechanism based on time-varying mask enhancement was proposed. Different from the traditional multi-head attention mechanism, the proposed time-aware multi-head attention mechanism can allocate the optimal attention calculation scheme according to the time characteristics of the input data, so as to more accurately model the time dependence relationship between different traffic nodes in the road network. The time-varying mask was composed of two parts: the static mask was embedded to correct the multihead attention, and the dynamic mask was embedded to enhance the time-sensing ability of the time-head attention.
- A novel graph learning strategy was proposed, which can learn static spatial association and dynamic spatial association in parallel. In order to learn the static spatial correlation better, the defined global embedding vector and local embedding vector were used to learn the spatial correlation of the road network at each time step, and a coupled graph learning mechanism was designed to couple the graphs learned at each time step. In order to model the dynamic spatial correlation in the road network more accurately, a mask based on topological matrix and semantic matrix was defined for the first time. Meanwhile, the mask was used to optimize the dynamic graph generated by the graph learning strategy.
- Simulation test results based on four real data sets verify the effectiveness of the proposed method HTVGNN.
 Compared with the latest space-time graph neural net-

work model, the proposed HTVGNN algorithm has higher prediction accuracy. In addition, the ablation experiment verifies that the coupled graph learning mechanism in the proposed graph learning strategy can effectively improve the long-term prediction performance of the model.

II. RELATED WORK

A. Traditional Traffic Forecasting Methods

Traffic flow prediction plays a pivotal role in urban intelligent transportation, enabling the anticipation of future traffic conditions based on real-time data from the traffic network. This information serves as a foundation for scheduling and decision-making by the traffic management department [18]. In earlier studies, researchers predominantly relied on mathematical statistical methods and early machine learning techniques, such as historical average (HA) [12] [11], autoregressive integrated moving average (ARIMA) [10] [11], vector autoregressive model (VAR) [19], etc. However, these models often underperform in actual traffic prediction tasks due to the complex and dynamic nature of traffic flow. With significant advancements in deep learning across various domains like speech recognition and image processing, an increasing number of researchers have started employing deep learning approaches for spatio-temporal traffic flow prediction tasks. Convolutional Neural Networks (CNN) [10], Long Short-Term Memory (LSTM) networks [9] along with its variant Gate Recurrent Unit (GRU) [9] are widely used and representative deep learning methods that have significantly enhanced the accuracy of traffic flow prediction. Unlike previous methods, deep learning-based approaches can effectively capture spatio-temporal correlations. For instance, Fully Connected Long Short-Term Memory Network (FC-LSTM) [20] combines CNN and LSTM to extract implicit spatio-temporal characteristics present in traffic flow data. Nevertheless, since CNN was originally designed to process Euclidean data with regular grid structures like images and videos rather than road networks' spatial features accurately; FC-LSTM's predictive performance is suboptimal.

B. Spatio-temporal graph neural network Traffic Forecasting Methods

Traditional traffic research considers traffic flow prediction as a simple time series problem, neglecting the influence of other nodes in the traffic network on the current node. Consequently, the performance of traditional prediction methods is suboptimal. To enhance modeling capabilities, researchers have started investigating effective approaches to capture spatial features within traffic networks. For instance, Conv-LSTM [21] employs convolution operations to model spatial features in sequences. However, conventional convolutional neural networks (CNNs) were originally designed for processing Euclidean data with regular grid structures like images and videos, making them ineffective for graph-structured data processing. Graph Convolutional Networks (GCNs) extend traditional convolutions to handle non-Euclidean data and have demonstrated promising results across various graph-based

prediction tasks. Spatio-temporal Graph Neural Networks (STGNNs), such as STGCN [14], are increasingly studied in traffic flow prediction research. STGCN combines graph convolutions with time convolutions or recurrent neural networks (RNNs), effectively capturing both spatial and temporal features within road networks. However, its ability to capture spatial features is limited by predefined graph structures used during training. In contrast, models like GraphWaveNet [22] and AGCRN [16] adaptively learn the graph structure of road networks from data without prior knowledge and achieve comparable prediction performance to models based on predefined graphs.

C. Transformer

The Transformer model was initially proposed in the field of machine translation [23] and has since been widely adopted in deep learning domains, including NLP [24] and computer vision [25]. It is a codec structure implemented with multihead self-attention (MSA), which exhibits strong modeling capabilities for contextual information. Consequently, MSA has found extensive applications in machine translation tasks, delivering superior performance. In the context of traffic flow prediction tasks, the Transformer model incorporates a time-based multi-head attention mechanism that maps data to high-dimensional space using multiple groups of attention mechanisms. This enables simultaneous learning of optimal attention between different features. Researchers have successfully introduced MSA into traffic flow prediction, yielding significant improvements across various aspects. For instance, Yan et al. [26] proposed the Traffic Transformer model by first employing a designed coding and embedding block to address data discrepancies across different research fields. Additionally, they enhanced the original encoder-decoder structure of Transformer by introducing two components: global encoder and global-local decoder blocks. These blocks are stacked together to form a deep prediction network with hierarchical characteristics. Wang et al. [27], on the other hand, presented a novel graph neural network layer incorporating position-wise attention mechanism that dynamically aggregates historical traffic flow information from adjacent roads. To better capture temporal features at both local and global levels, they combine RNN with a Transformer layer.

III. METHODOLOGY

A. Problem defination

Definition 1. **Traffic Network**: The traffic network can be represented as a weighted directed graph $\mathcal{G}=(\mathcal{V},\mathcal{E},A)$, where \mathcal{V} represents all nodes (sensors) in the road network) $(|\mathcal{V}|=N)$, \mathcal{E} is the set of all edges, which represents the connectivity between nodes. $A\in R^{N\times N}$ represents the weighted adjacency matrix, and its value represents the connectivity between nodes. degree of correlation.

Definition 2. **Traffic Flow Characteristics**: Based on the transportation network, we define the problem of traffic flow prediction with input $X \in \mathbb{R}^{N \times d}$ represents the traffic flow characteristics observed by all nodes at a certain time (such as traffic flow, speed, etc.)

Definition 3. **Traffic Prediction**: Given the road topology $\mathcal G$ and traffic characteristics X. Our goal is to predict the future traffic conditions $P = [P_{t+1},...,P_{t+\tau}] \in R^{\tau \times N \times C}$ at τ times by analyzing the data $X = [X_{t-T+1},...,X_t] \in R^{T \times N \times C}$ at T times in the past.

Definition 4. **Time-varing Mask Embeding**: If there are N nodes in the traffic network, and the sensor in the network sampling d times per day. The week consists of a total of 7 days. Then the static mask embedding and dynamic mask embedding can be represented by three independent trainable sub-mask embeddings $\tilde{E} \in R^{N \times d_m}$ and $\tilde{E}_D \in R^{D \times d_m}$, $\tilde{E}_W \in R^{W \times d_m}$. d_m represents the dimension of sub-mask embedding.

IV. HYBRID TIME-VARYING GRAPH NEURAL NETWORK

The present study proposes a time trend-aware multi-head self-attention transformer and a graph convolution GRU-based traffic flow prediction model. The former effectively captures local temporal features, while the latter simultaneously extracts spatio-temporal features. Firstly, we introduce the fundamental structure of HTVGNN and illustrate it in Fig. 1. To better represent intricate correlations among nodes, we propose static and dynamic time-varing graphs that learn changing spatial correlations through trainable node embeddings. Subsequently, graph convolution GRU is employed to extract spatio-temporal features for accurate traffic flow prediction. Detailed model structures and mechanisms are presented in subsequent subsections.

A. An enhanced temporal perception multi-head self-attention

Self-attention mechanism is a broader attention mechanism where query, key and value are different representations of the same sequence. In order to learn the complex and time-varying temporal dependencies of input data, the temporal feature $X \in R^{N \times C}$ is usually mapped to a high-dimensional space with a widely used multi-head self-attention (MHSA) [1]. For the i^{th} self-attention head at time step t, $Q_i \in R^{N \times d_q}$, $K_i \in R^{N \times d_k}$ and $V_i \in R^{N \times d_v}$ are generated by the linear projection as defined in Eq. (1), respectively.

$$Q_i = XW_i^q,$$

$$K_i = XW_i^k,$$

$$V_i = XW_i^v,$$
(1)

where W_i^q , W_i^k , and W_i^v are learnable parameters of the i^{th} self-attention head.

Then, $Q_i \in R^{N \times d_q}$, $K_i \in R^{N \times d_k}$ and $V_i \in R^{N \times d_v}$ are input into a parallel attention score function as defined in Eq.(2) to calculate the attention of the i^{th} self-attention head $head_i$.

$$head_{i} = Attention (Q_{i}, K_{i}, V_{i})$$

$$= Softmax \left(\frac{Q_{i}K_{i}}{\sqrt{d_{head}}}\right) V_{i},$$
(2)

Finally, the final multi-head self-attention corresponding to the input $X \in \mathbb{R}^{N \times C}$ can be obtained by weighting the

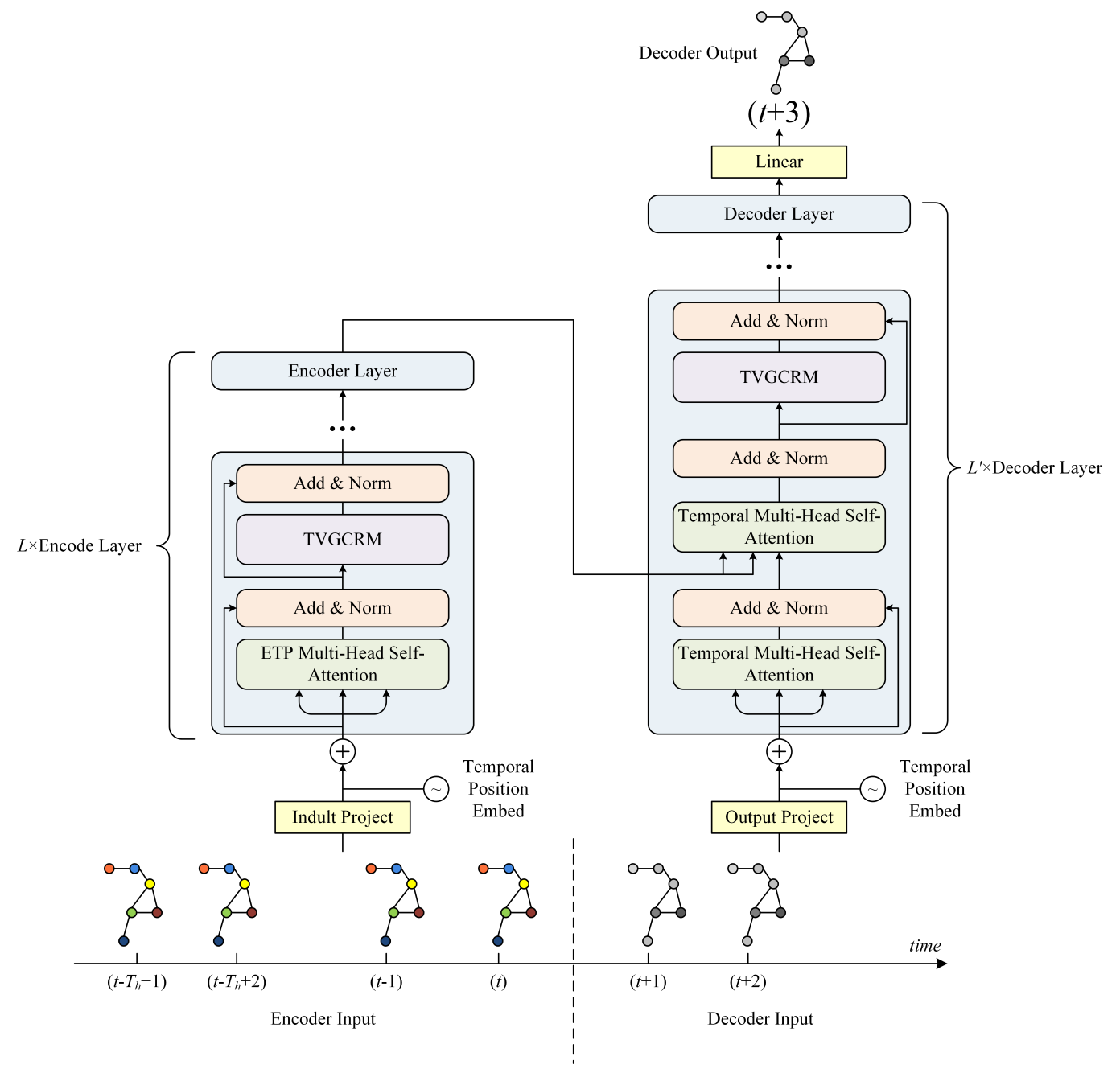


Fig. 1. The diagram of the overall architecture of the HTVGNN.

attention of the h self-attention heads together. Specifically, it can be calculated by the following Eq. (3),

$$MHSA = [head_1, \cdots, head_i, \cdots, head_h]W,$$
 (3)

where h is the total amount of attention heads. W is the final output projection matrix. However, in traditional multihead attention mechanism, the Key vectors (K_i) will cause unnecessary interference [Weiguo Zhu]. In addition, since the learned matrix W_i^q , W_i^k , and W_i^v are static, the score calculated by the traditional multi-head attention equation defined in Eq. (2) can not fully perceive the temporal trend of self-attention. Therefore, we have proposed an enhanced temporal perception multi-head self-attention. For notational

simplicity, our proposed enhanced temporal perception multihead self-attention (ETPMSA) as shown in Fig.2, ETPMSA can be calculted by the following as Eq.(4):

$$\begin{split} ETPMulAtt(Q,K,V) &= \Theta \cdot \widehat{W}, \\ \Theta &= [head_1^{ETP}, \cdots, head_i^{ETP}, \cdots, head_h^{ETP}], \end{split} \tag{4}$$

where \widehat{W} is a learnable parameter vector, $head_i^{ETP}$ denotes the i^{th} self-attention head which can be calculted by the following Eq. (5).

$$head_i^{ETP} = Softmax\left(\frac{Q_i \cdot K_i^{ETP}}{\sqrt{d_{head}}}\right) V_i$$
 (5)

$$K_i^{ETP} = M \odot K_i, \tag{6}$$

$$M_t = Softmax(Relu(m_t \cdot m_t^T)), \tag{7}$$

$$m_t = \tilde{E} \odot \tilde{P}_D \odot \tilde{P}_W, \tag{8}$$

where $Q_i \in R^{N \times d_q}$, $K_i \in R^{N \times d_k}$ and $V_i \in R^{N \times d_v}$ are the Query, Key and Value of the traditional time multi-head attention as defined in Eq. (2), $M_t \in R^{N \times N}$ is adaptive mask matrix which is defined according to the size of the input data. It should be noted that, $m \in R^{T \times N \times d_m}$ is the mask embedding which composed by three submask embedding $\tilde{E} \in R^{N \times d_m}$, $\tilde{P}_D \in R^{N \times d_m}$, $\tilde{P}_W \in R^{N \times d_m}$. Herein, submask embedding \tilde{E} is defined to enhance the accuracy of multi-head self-attention. submask embedding \tilde{P}_R , \tilde{P}_D are daily mask embedding and weekly mask embedding whose time step is constitent with the history data X.

B. Time-varying graph convolution recurrent module

The architecture of our proposed TVGCRM is illustrated in Fig. 3. The details of the TVGCRM is summarized as follows.

1) Graph learning: There usually exist static and dynamic spatial correlations between different traffic nodes. In order to capture the static and dynamic spatial correlations, we have proposed a graph learning method to generate static graph and dynamic graph in a data-driven manner without providing any prior knowledge.

• Static graph learning.

In order to capture the static spatial correlations between traffic nodes, we use two learnable embedding vectors to adaptively learn the static adjacency matrix at each time step. The static adjacency matrix A_k^s of the k^{th} time step is defined as follows:

$$E_k = E + e_k$$

$$A_k^s = Softmax(Relu(E_k \odot E_k^T))$$
(9)

where E is a trainable node embedding, e_k is a trainable bias of the node embedding E. Herein, in order to ensure the diversity of A_k^s at different time step, we set different bias e_k for different time step k^{th} during the training process, Relu() is used as the activation function.

In order to model the similarity of traffic flow between different traffic nodes, a traffic pattern graph is defined by calculating the correlations of historical traffic flows using the DTW algorithm [28]. In general, traffic pattern graph reflects a long-term traffic pattern. However, short-term traffic pattern may play an more important role in short-term traffic flow prediction. Therefore, in order to obtain more spatial topology-related information at different time step, we have proposed a static graph learning module to improve the learning ability of the static adjacency matrix. At each time step, we can construct a static graph with the static adjacency matrix A_t^s defined in Eq.(9). Then, in order to more accurately model static spatial correlations between different traffic nodes, we can further calculate the coupling time-varing adjacency matrix by the

following Eq.(10):

$$A_{0}^{s} = SoftMax(Relu(E_{0} \odot E_{0}^{T}))$$

$$A_{1}^{s} = [A_{0}^{s}||SoftMax(Relu(E_{1} \odot E_{1}^{T}))] \odot W_{1}$$

$$\vdots$$

$$A_{12}^{s} = [A_{0}^{s}||A_{1}^{s}||...||A_{1}0^{s}||SoftMax(Relu(E_{11} \odot E_{11}^{T}))] \odot W_{11}$$

$$(10)$$

where || is the concate operation, W_0, W_1, W_{11} are learnable parameter matrices after completing the graph coupling process, we substitute the time-varying graph in A^s at each corresponding time step with the coupled graph as the final A^s .

• Dynamic graph learning.

In order to capture the dynamic spatial correlations between different traffic nodes, the dynamic adjacency matrix is calculated based on the hidden embedding H of current traffic features. Herein, we design a 1×1 convolution layer as the mapping function ϕ . The mapping processing can be defined by the Eq.(11). Then, a learnable vector a is defined to calculate the attention weight between node i and node j.

the dynamic adjacency matrix $\tilde{A}^v_{k_{(i,j)}}$ at the k^{th} time step between node i and node j is defined as Eq. (11) to Eq.(14)

$$E_k^v = H_k W_\phi \tag{11}$$

$$e_{ij}^{v} = a \cdot ([E_{k}^{v}]_{i} || [E_{k}^{v}]_{j})$$
 (12)

where H_k is the value of the hidden embedding $H \in R^{T \times N \times C_\phi}$ at time step $t.E_k^v \in R^{N \times d_\phi}$ is the mapped traffic features including short-term dynamic spatial traffic patterns implicit in current traffic features X. $[E_k^v]_i$ is the i-th node in $E_k^v.$ || represents a splicing operation. e_{ij}^v Indicates the dynamic traffic similarity between node i and node j in the road network.

Then, using Softmax() for normalization, the generation process of $A^v_{k_{(i,j)}}$ is as Eq. (13):

$$A_k^v(i,j) = \left[Softmax(e_{i,:}^v)\right]_i \tag{13}$$

Then,we think dynamic changes of spatial correlations occuring in the current time should belong to the most active nodes. such as nodes which lied in adjency matrix and DTW matrix.thus,we combine the adjency matrix and DTW matrix as the mask matrix of dynamic spatial correlations. Finally the dynamic adjacency matrix $\tilde{A}^{v}_{k(i,j)}$ can be define as Eq. (14):

$$\tilde{A}_{k_{(i,j)}}^{v} = A_{k_{(i,j)}}^{v} \odot (A + A_{dtw})$$
 (14)

2) Time-varying graph convolution gated recurrent unit: GRU is a variant of RNN which maintains the effectiveness of RNN in capturing temporal features while simplifying the parameters of the model, making it widely used in capturing temporal correlation. Draw inspiration from previous studies [29] [30], we modify the MLP layer in GRU with the proposed TVGCN model, and combine TVGCN and GRU to capture Spatio- temporal dependencies between different nodes. The

specific form can be defined as Eq. (15):

$$z^t = \sigma(|| \left[\mathcal{G}_s([H^{(t)}||h^{(t-1)},E];\theta_{z_1}), \mathcal{G}_d([H^{(t)}||h^{(t-1)},E^v];\theta_{z_2}) \right]^{\text{the traffic condition Modeled as a seasonal process and using historical averages as forecast.}$$

$$r^t = \sigma(|| \left[\mathcal{G}_s([H^{(t)}||h^{(t-1)},E];\theta_{r_1}), \mathcal{G}_d([H^{(t)}||h^{(t-1)},E^v];\theta_{r_2}) \right]^{\bullet} \text{ Vector Auto Regression (VAR) [6]VAR model can handle time series models of correlations between multiple variables.}$$

$$c^t = \tanh(|| \left[\mathcal{G}_s([H^{(t)}||g^t,E];\theta_{c_1}), \mathcal{G}_d([H^{(t)}||g^t,E^v];\theta_{c_2}) \right]) \text{ variables.}$$

$$g^t = r^t \odot h^{(t-1)}$$

$$h^t = z^{(t)} \odot h^{(t-1)} + (1-z^{(t)}) \odot c^t \text{ time series forecasting.}$$

$$\bullet \text{ Spatial- temporal graph convlutional networks}$$

where $H^{(t)}$ and $h^{(t)}$ are the input hidden embedding and output hidden embedding at $t^t h$ time step. || represents the concatenation operation. z^t and r^t represent reset gate and update gate at t time steps respectively. \mathcal{G}_s and \mathcal{G}_d represent the static graph operation and dynamic graph operation severally. $\theta_{z_1}, \theta_{z_2}$ and θ_{r_1} , θ_{r_2} and θ_{c_1} , θ_{c_2} are learnable parameters in TVGCRM

C. Position Encodings

Temporal position coding is employed to represent the temporal order within a time series, where sequences of consecutive time steps exhibit higher correlation. In the conventional Transformer model, sine and cosine functions are utilized for mapping different feature dimensions during the calculation process of temporal position encoding, as formulated in Eq. (16).

$$PE(pos, 2d) = sin\left(\frac{pos}{10000^{\frac{2d}{d_{model}}}}\right)$$

$$PE(pos, 2d+1) = cos\left(\frac{pos}{10000^{\frac{2d}{d_{model}}}}\right)$$
(16)

Among them, pos represents the position and d represents the feature dimension.

V. EXPERIMENTS

A. Datasets

We validate the predictive performance of HTVGNN by conducting experiments on four real-world traffic datasets, namely PeMSD3, PeMSD4, PeMSD7, and PeMSD8. These datasets were collected by the California Department of Motor Transportation Performance Measurement System (PeMS) [39]. Please refer to Table ?? for detailed information.

B. Evaluation Metrics

In this study, we employed three effectiveness measures, namely Mean Absolute Error (MAE), Mean Absolute Percentage Error (MAPE), and Root Mean Square Error (RMSE), to assess the accuracy of the HTVGNN model as described in Eq. 20 through 22.

C. Baselines

We compare the HTVGNN model against fourteen state-ofthe-art baselines as outlined below:

- Historical Average (HA) [31] The HA model takes 1the traffic condition Modeled as a seasonal process and using
- variables.
- Long Short Term Memory (LSTM) [20] LSTM is a classical variant of RNN, and it can be used for long-term time series forecasting.
- Spatial- temporal graph convlutional networks (STGCN) [14]STGCN is a novel spatio-temporal graph convolutional network that effectively captures both spatial and temporal features through the integration graph convolution and gated time convolution.
- Diffusion Convolutional Recurrent Neural Network (DCRNN) [32] DCRNN models the spatial dependency by relating traffic flow to a diffusion process, and introduce diffusion convolution into GRU in an encoder-decoder manner for multi-step traffic flow forecasting.
- Graph WaveNet(GWN) [22] Graph WaveNet for Deep Spatial-Temporal Graph Modeling uses adaptive adjacency matrices and learns by node embedding. Temporal dependence captures using 1D dilated convolution.
- Attention Based Spatial-Temporal Graph Convol utional Network (ASTGCN) [33] ASTGCN introduces attention mechanisms into CNN and GCN to respectively model spatial and temporal dynamics of traf?c data.
- Adaptive Graph Convolutional Recurrent Network (AGCRN) [29] AGCRN utilizes a node adaptive parameter learning to enhance GCN and combines it with GRU to capture spatial and temporal features of traf?c data.
- A Graph Multi-Attention Network for Traffic **Prediction** (GMAN) [34] use a spatial-temporal fusion module that a new graph structure constructs based on a datadriven.
- Learning Dynamic and Hierarchical Traffic Spatio temporal Features With Transformer (Tformer) [35] which designs an encode-decoder architecture to consistently model the spatial and temporal dependencies in the traffic timeseries by GCN and transformer, respectively approach Dual Dynamic Spatial-Temporal Graph Convolution Network for Traffic Prediction.
- Dual Dynamic Spatial-Temporal Graph Convolution **Network for Traffic Prediction (DDSTGCN)** [36] LSTM is used to encode historical stream data, and a global encoder and a global-local decoder are designed to extract global and local spatial correlations.
- Delay-Aware Dynamic Long-Range Transformer for Traffic Flow Prediction (PDFormer) [37] The k-Shape algorithm is used to classify regional nodes to model the delay between different nodes, thereby constructing a short-range graph mask matrix. In addition, DTW is used to construct another long-range graph mask matrix. On this basis, a split spatio-temporal multi-head attention mechanism is designed to model short-range spatial dependence, longrange spatial dependence and time dependence respectively.
- Bidirectional Spatial-Temporal Adaptive Transfor mer for Urban Traffic Flow Forecasting (Bi-STAT [38] The

TABLE I. Evaluation results of each model under different prediction steps

| D.4. M. 1.1 | | | 15min | | 30min | | 60min | | Average | |
|-------------|---------------|-------|--------|--------------|--------|------------|----------|-------------------|---------|-------|
| Data | Model | MAE N | MAPE(% |)RMSE MAE | MAPE(% |)RMSE MA | E MAPE(% | RMSE MAE | MAPE(% |)RMSE |
| | HA [31] | 23.57 | 22.13 | 36.48 27.51 | 29.14 | 44.99 40.1 | 11 39.10 | 61.16 30.03 | 28.63 | 47.17 |
| | VAR [6] | 17.41 | 18.20 | 25.42 22.13 | 24.28 | 32.20 31.6 | 55 37.42 | 44.89 22.91 | 25.53 | 33.04 |
| | LSTM [20] | 16.69 | 16.02 | 25.54 20.03 | 19.34 | 30.40 27.4 | 12 29.48 | 40.20 20.64 | 20.57 | 31.63 |
| | DCRNN [32] | 15.45 | 14.98 | 25.75 17.98 | 17.38 | 29.80 23.1 | 12 22.54 | 37.18 18.31 | 17.74 | 30.08 |
| | STGCN [14] | 18.46 | 19.56 | 31.27 19.55 | 22.74 | 32.59 21.7 | 70 24.08 | 35.29 19.64 | 21.63 | 32.74 |
| PEMS03 | GWN [22] | 16.06 | 15.39 | 27.38 19.25 | 18.45 | 32.29 26.1 | 12 26.32 | 41.89 19.82 | 19.21 | 32.88 |
| | ASTGCN [33] | 15.24 | 15.31 | 25.25 14.63 | 16.71 | 15.65 27.6 | 54 20.25 | 18.63 16.96 | 15.97 | 28.15 |
| | AGCRN [29] | 14.61 | 13.82 | 25.84 15.65 | 14.61 | 27.51 17.4 | 15.94 | 30.23 15.70 | 14.66 | 27.63 |
| | GMAN [34] | 15.65 | 16.68 | 26.09 16.32 | 16.32 | 27.15 17.7 | 73 18.91 | 29.26 16.45 | 17.47 | 27.31 |
| | Tformer [35] | 14.97 | 15.63 | 23.86 16.54 | 17.15 | 26.22 19.0 | 08 19.49 | 29.57 16.54 | 17.15 | 26.25 |
| | DDSTGCN [36] | 13.70 | 13.99 | 23.95 14.88 | 14.91 | 25.38 16.8 | 38 16.63 | 29.13 14.93 | 14.96 | 25.83 |
| | PDFormer [37] | 13.73 | 13.60 | 24.84 14.99 | 14.13 | 26.58 17.1 | 14 16.31 | 29.43 15.02 | 14.35 | 26.63 |
| | Bi-STAT [38] | 14.30 | 14.78 | 25.07 15.43 | 15.67 | 26.93 17.1 | 19 17.21 | 29.57 15.47 | 15.74 | 26.92 |
| | HTVGNN | 13.20 | 13.76 | 22.9314.36 | 14.52 | 24.8115.9 | 92 15.67 | 27.1514.24 | 14.36 | 24.63 |
| | HA [31] | 30.70 | 20.71 | 45.02 37.47 | 27.10 | 54.37 50.8 | 38.58 | 72.67 38.56 | 28.17 | 56.85 |
| | VAR [6] | 22.75 | 16.95 | 33.11 27.93 | 22.10 | 39.68 38.2 | 26 32.74 | 52.57 28.78 | 23.01 | 40.72 |
| | LSTM [20] | 21.89 | 14.79 | 33.01 25.98 | 18.07 | 38.65 35.1 | 12 27.28 | 50.35 26.81 | 19.28 | 40.18 |
| | DCRNN [32] | 20.61 | 13.91 | 32.224 23.87 | 16.18 | 36.80 30.8 | 33 21.27 | 46.27 24.44 | 16.64 | 37.48 |
| | STGCN [14] | 23.43 | 20.43 | 35.30 25.45 | 22.56 | 37.83 30.4 | 15 27.84 | 44.12 25.91 | 22.90 | 38.44 |
| | GWN [22] | 20.90 | 14.44 | 33.04 24.53 | 17.45 | 38.22 32.5 | 58 23.38 | 49.15 25.25 | 18.22 | 39.10 |
| | ASTGCN [33] | 19.55 | 12.99 | 31.16 20.32 | 13.39 | 32.39 23.6 | 53 15.31 | 37.21 20.59 | 13.53 | 32.85 |
| | AGCRN [29] | 18.88 | 12.49 | 30.92 19.65 | 12.94 | 32.29 21.3 | 34 13.87 | 34.98 19.76 | 12.99 | 32.48 |
| | GMAN [34] | 18.54 | 12.99 | 29.74 19.09 | 13.47 | 30.70 20.9 | 92 15.12 | 33.24 19.34 | 13.71 | 30.98 |
| | Tformer [35] | 21.02 | 14.94 | 31.33 22.37 | 16.24 | 33.05 23.7 | 72 17.41 | 34.73 21.10 | 15.13 | 31.46 |
| | DDSTGCN [36] | 18.40 | 12.86 | 29.38 19.64 | 13.77 | 31.15 21.8 | 32 15.40 | 34.07 19.74 | 13.83 | 31.12 |
| | PDFormer [37] | 18.12 | 12.41 | 29.02 19.23 | 13.39 | 30.60 21.2 | 26 14.86 | 33.36 19.30 | 13.30 | 30.67 |
| | Bi-STAT [38] | 18.16 | 12.39 | 29.29 19.01 | 12.92 | 30.61 21.6 | 58 15.36 | 33.85 19.66 | 13.02 | 30.64 |
| | HTVGNN | 17.38 | 11.47 | 28.5318.18 | 11.93 | 29.86 19.4 | 11 12.74 | 31.6818.15 | 11.92 | 29.79 |

encoder-decoder structure consists of a temporal Transformer and a spatial Transformer. The difference is that a recall module is added to the decoder to provide supplementary information for the prediction task. The designed DHM module is used to dynamically adjust the complexity of the model according to the complexity of the prediction task.

D. Hyperparameter setting

1) Dataset Preprocessing: Following recent methodologies [40], [41] and [42], we partition the training, validation, and test sets in a 6:2:2 ratio. To ensure more stable training, we employ z-score standardization. Additionally, we utilize historical traffic flow speed data from the past T=12 time slices (60 min) to predict future traffic flow speed in $\tau=12$ time slices (60 min). The input data is normalized using Z-Score as shown in Eq. (17).

$$\widehat{x} = \frac{x - mean(x_{trian})}{std(x_{train})}$$
 (17)

Among them, mean() and std() represent the mean and standard deviation functions, and x_{trian} represents the training set.

2) Model Settings: The experiments were conducted on a machine equipped with dual NVIDIA RTX and 32GB of memory. HTVGNN was implemented using Ubuntu 18.04, PyTorch 2.0.0, and Python 3.9.7, with a hidden dimension E of 64, eight heads for the Transformer, and two layers for GRU. The optimal model was determined based on performance on the validation set, trained using Adam optimizer [43] with a learning rate of 0.001 over a batch size of 32 for training epoch of up to 300.

E. Performance Comparison

Tables I and II present the comparison results of 12 prediction models on four datasets. Overall, our HTVGNN achieved exceptional prediction accuracy across all 12 prediction strides. The deep learning-based approaches outperformed traditional statistical-based approaches (VAR), indicating their efficacy in modeling highly nonlinear traffic flows. As depicted in Tables I and II, these approaches exhibited suboptimal prediction performance. Moreover, methods that capture spatiotemporal dependencies generally surpassed those solely modeling temporal dependencies (LSTM), underscoring the

TABLE II. Evaluation results of each model under different prediction steps

| Data | Model | | 15min | | | 30min | | | 60min | | | Average | |
|--------|---------------|-------|---------|-------|-------|---------|-------|-------|---------|-------|-------|---------|-------|
| Data | | MAE N | MAPE(%) | RMSE | MAE | MAPE(%) | RMSE | MAE | MAPE(%) | RMSE | MAE | MAPE(%) | RMSE |
| | HA [31] | 35.67 | 16.49 | 52.07 | 44.06 | 20.82 | 64.02 | 60.44 | 29.69 | 87.05 | 45.36 | 21.59 | 67.17 |
| | VAR [6] | 25.10 | 10.86 | 37.22 | 31.30 | 14.08 | 45.23 | 42.96 | 42.96 | 60.04 | 32.03 | 14.61 | 46.12 |
| | LSTM [20] | 23.66 | 10.48 | 35.77 | 28.50 | 12.76 | 42.67 | 39.12 | 18.66 | 56.60 | 29.32 | 13.30 | 44.39 |
| | DCRNN [32] | 21.97 | 9.42 | 33.94 | 25.68 | 11.14 | 39.16 | 33.29 | 14.93 | 49.09 | 26.15 | 11.44 | 39.57 |
| | STGCN [14] | 32.52 | 16.23 | 51.71 | 33.26 | 16.25 | 52.75 | 36.02 | 17.59 | 55.64 | 33.62 | 16.53 | 53.04 |
| PEMS07 | GWN [22] | 21.72 | 9.52 | 34.78 | 25.89 | 11.89 | 41.05 | 34.83 | 16.78 | 53.72 | 26.58 | 12.28 | 41.85 |
| | ASTGCN [33] | 23.94 | 10.25 | 36.88 | 28.77 | 12.50 | 43.89 | 39.37 | 18.00 | 58.07 | 29.59 | 13.04 | 45.52 |
| | AGCRN [29] | 19.89 | 8.34 | 32.68 | 21.29 | 8.93 | 34.91 | 23.51 | 9.85 | 38.45 | 21.26 | 8.91 | 34.99 |
| | GMAN [34] | 19.08 | 8.11 | 31.23 | 20.23 | 8.57 | 33.37 | 22.30 | 9.56 | 36.58 | 20.35 | 8.65 | 33.39 |
| | Tformer [35] | 20.28 | 9.07 | 31.31 | 22.10 | 10.08 | 34.19 | 25.15 | 11.87 | 38.52 | 22.07 | 10.12 | 34.21 |
| | DDSTGCN [36] | 19.72 | 8.82 | 31.83 | 27.42 | 11.87 | 41.87 | 24.49 | 10.91 | 39.03 | 21.55 | 9.59 | 34.65 |
| | PDFormer [37] | 20.58 | 8.76 | 32.50 | 22.72 | 9.77 | 35.71 | 24.77 | 10.33 | 40.55 | 21.98 | 9.17 | 36.03 |
| | Bi-STAT [38] | 19.66 | 8.36 | 31.81 | 21.44 | 9.07 | 34.70 | 24.34 | 10.43 | 38.88 | 21.50 | 9.15 | 34.64 |
| | HTVGNN | 17.99 | 7.60 | 30.00 | 19.52 | 8.15 | 32.65 | 21.86 | 9.21 | 36.20 | 19.46 | 8.15 | 32.53 |
| | HA [31] | 25.15 | 15.76 | 37.00 | 31.09 | 19.62 | 45.32 | 42.92 | 27.66 | 61.42 | 32.06 | 20.35 | 47.52 |
| | VAR [6] | 17.88 | 12.17 | 26.48 | 22.21 | 15.50 | 32.39 | 30.63 | 21.94 | 42.92 | 22.81 | 15.96 | 32.97 |
| | LSTM [20] | 17.71 | 11.58 | 26.65 | 21.31 | 14.83 | 31.97 | 29.37 | 19.62 | 42.53 | 21.96 | 14.52 | 33.22 |
| | DCRNN [32] | 15.93 | 10.05 | 24.62 | 18.30 | 11.57 | 28.43 | 23.02 | 14.42 | 35.05 | 18.59 | 11.72 | 28.64 |
| | STGCN [14] | 20.53 | 14.25 | 29.92 | 22.21 | 16.23 | 32.24 | 26.40 | 21.17 | 37.37 | 22.62 | 16.52 | 32.66 |
| | GWN [22] | 15.59 | 9.84 | 25.27 | 18.28 | 12.06 | 30.02 | 24.18 | 15.63 | 38.85 | 18.75 | 12.12 | 30.47 |
| | ASTGCN [33] | 16.36 | 10.01 | 25.24 | 18.38 | 11.12 | 28.34 | 22.60 | 13.57 | 34.39 | 18.61 | 11.27 | 28.82 |
| | AGCRN [29] | 14.90 | 9.67 | 23.39 | 15.90 | 10.26 | 25.18 | 17.84 | 11.37 | 28.32 | 16.01 | 10.31 | 25.36 |
| | GMAN [34] | 13.75 | 9.07 | 22.84 | 14.16 | 9.35 | 23.74 | 15.47 | 10.40 | 25.72 | 14.32 | 9.50 | 23.89 |
| | Tformer [35] | 15.41 | 10.14 | 22.98 | 16.83 | 11.77 | 25.11 | 19.08 | 12.61 | 28.19 | 16.79 | 11.41 | 25.11 |
| | DDSTGCN [36] | 14.31 | 9.71 | 22.45 | 15.44 | 10.39 | 24.42 | 17.42 | 11.61 | 27.33 | 15.49 | 10.42 | 24.36 |
| | PDFormer [37] | 14.08 | 8.98 | 22.29 | 15.19 | 9.96 | 24.27 | 16.98 | 11.04 | 27.06 | 15.20 | 9.81 | 24.18 |
| | Bi-STAT [38] | 13.92 | 9.02 | 22.32 | 14.64 | 9.52 | 23.75 | 16.14 | 10.59 | 26.11 | 14.76 | 9.62 | 23.80 |
| | HTVGNN | 12.59 | 8.16 | 21.10 | 13.44 | 8.73 | 22.87 | 14.73 | 9.62 | 25.03 | 13.44 | 8.74 | 22.78 |

significance of spatial dependencies. DCRNN and STGCN employ predefined graphs to model spatial dependencies in road networks; however, their performance heavily relies on the quality of these predefined graphs. AGCRN utilizes adaptive graphs to capture spatial dependencies, which typically enhances predictions compared to predefined graphs. Nevertheless, both predefined and adaptive graphs remain static during the prediction stage, disregarding dynamic changes in the road network. In contrast, models that dynamically model spatial dependencies (GMAN, PDFormer) significantly outperform other approaches based on static graph structures (DCRNN, STGCN, GWN). This can be attributed to their ability to learn dynamically changing graph structures and provide a broader representation space for modeling more complex spatiotemporal dependencies. Compared to other models, HTVGNN incorporates a time-varying mask matrix to enhance the multi-head attention mechanism for accurately capturing dynamic temporal correlations. Moreover, HTVGNN employs a dedicated coupled graph learning method tailored for multihead attention, effectively improving its performance in longterm prediction tasks. Additionally, to better model dynamic spatial correlations in road networks, we define a mask based

on topological and semantic matrices to optimize the dynamic time-varying graphs. Overall, our model outperforms existing state-of-the-art approaches on four datasets, achieving superior prediction accuracy.

Additionally, in order to demonstrate the overall superiority of our model, we provide visual representations for each prediction point of HTVGNN and 11 comparative models as depicted in Fig. 4. In terms of the PEMS03 and PEMS04 datasets, our model exhibits the smallest cumulative error as the time steps increase, highlighting a distinct advantage of HTVGNN during long-term prediction stages. Furthermore, for PEMS07 and PEMS08 datasets, our model consistently maintains a significant advantage across all time steps.

F. Abliation sudy

The purpose of this section is to demonstrate the efficacy of the key components in our model through a series of experiments. The subsequent variations aim to indicate the effectiveness of different combinations of modules:

w/o ETPMSA: TVGCRM should be utilized exclusively, with the exclusion of the enhanced temporal perception multi-

head self-attention mechanism. This variant primarily demonstrates the function of the enhanced temporal perception multihead self-attention.

w/o TV: Replace the time-varying graph in TVGCRM with a topological graph, emphasizing its pivotal role in capturing temporal dynamic correlations.

w/o TR: Replace TVGCRM with a topological graphbased graph convolution, which primarily emphasizes the role of the RNN module in HTVGNN. At this juncture, the number of layers remains unchanged.

The experiments were conducted multiple times, and the optimal MAE, RMSE, and MAPE values for each variant on PEMSD4 and PEMSD8 are presented in Table 4.

The results presented in Table 4 demonstrate the superior performance of HTVGNN without ETPMSA, highlighting the crucial role played by ETPMSA in HTVGNN. Furthermore, the inferior performance of w/o TV compared to HTVGNN indicates that capturing dynamic correlations through timevarying graphs is essential. Additionally, w/o TR being inferior to HTVGNN reveals the positive contribution of RNN in capturing temporal correlations.

Given that our model is a hybrid time-varying graph convolutional neural network, this tutorial aims to dissect the impact of time-varying embedding and time-varying mask embedding by dividing the model into modules, ultimately analyzing their influence on the model's performance.

1) Effect analysis of time-varying embedding in RTP multihead attention: We compare transformer modules based on enhanced temporal perception multi-head self-attention across different layers to analyze the performance improvement of the enhanced temporal perception multi-head self-attention Transformer, which utilizes an time-varing mask matrix, relative to the Transformer with temporal multi-head self-attention. Internally, our Transformer employs dynamic graph convolution based on topological graphs to capture dynamic spatial correlations. Prior to that, we investigate the impact of varying sizes of mask embedding and dropout on enhanced temporal perception multi-head self-attention. For this analysis, we set the number of layers to 1 and select optimal spatial embedding and dropout ratios. Fig. 6 illustrates how different time-varing mask embeddings and dropouts affect PEMS04 and PEMS08 datasets in terms of enhanced temporal perception multi-head self-attention.

To highlight the advantages of enhanced temporal perception in multi-head self-attention, we set the number of layers to 4 based on optimal mask embedding and dropout. We designed two variants as described below:

Transformer-o: Transformer with temporal multi-head attention.

Transformer-tv: A Transformer that calculates attention scores with our proposed spatiotemporal multi-head attention.

The results of the two variants with different numbers of layers are presented in Table 5. It is evident that Transformer-tv outperforms Transformer-o significantly when the number of layers is 1 and 4. Our proposed time-varying mask matrix effectively mitigates the issue of inaccurate calculation in multi-head self-attention, while greatly enhancing temporal perception capability.

2) Effect analysis of different types of graph structure in TVGCRM and HTVGNN: We have developed four variations of TVGCRM to underscore the significance of diverse manifestations of time-varying graphs, which are enumerated as follows:

TVGCRM: This is a coupled time-varying graph convolutional network.

TVGCRM-sl:Let different time slices be learned with different embeddings, but the spatial correlations learned in different time slices are not coupled.

TVGCRM-ag:: All time slices are learned using the same embedding, in which case the time-varying graph is the same as AGCRN.

TVGCRM-s:Replace coupled time-varying graphs with topological graphs.

The results presented in Table 6 unequivocally demonstrate the superiority of TVGCRM and its variants, namely TVGCRM-sl and TVGCRM-ag, over TVGCRM-s. This highlights the limitations of predefined graphs in accurately representing spatial correlations on traffic networks. Furthermore, the superior performance of TVGCRM-sl compared to TVGCRM-ag suggests that spatial correlations vary across different time steps, indicating that employing a single time-varying graph for learning is suboptimal. Moreover, the superiority of TVGCRM over TVGCRM-sl implies that considering the corresponding spatial correlations for different time steps is crucial as it allows capturing relevant information from other time steps to enhance modeling accuracy in current time steps.

Subsequently, we assess the impact of our proposed RTP multi-head self-attention and coupling time graph on the overall model performance by leveraging the aforementioned optimal mask embedding and dropout techniques. We devise a series of five variants to conduct ablation experiments on our model using PEMS04 and PEMS08 datasets. These variants aim to highlight the significance of time-varying mask embedding and time-varying embedding in our approach, as described below:

HTVGNN-tg: The time-varying mask embedding is excluded from the RTP multi-head attention, while TVGCRM remains unchanged as HTVGNN.

HTVGNN-wc: Remove the coupling part of the time-varying graph.

HTVGNN-sc: Simultaneously eliminate RTP multi-head self-attention and coupled time-varying graphs in a synchronized manner.

HTVGNN: This is a hybrid time-varying graph convolutional network, as shown in Fig. 1

The results presented in Table 7 demonstrate the superiority of HTVGNN over both HTVGNN-tg and HTVGNN-wc, highlighting the positive impact of incorporating timevarying mask embedding on enhancing self-attention accuracy. Furthermore, the superior performance of HTVGNN compared to HTVGNN-wc indicates its advantage in capturing spatial correlations in transportation networks by leveraging coupling time-varying graphs.

In particular, The ablation study revealed that our proposed HTVGNN, incorporating time-varying graphs, yields

| Dataset | Variants | | 15mi | in | | 30m | in | 60min | | |
|---------|-----------|-------|-------|---------|-------|-------|---------|-------|-------|---------|
| | | MAE | RMSE | MAPE(%) | MAE | RMSE | MAPE(%) | MAE | RMSE | MAPE(%) |
| PEMS04 | HTVGNN-wc | 17.49 | 28.67 | 11.55 | 18.59 | 30.49 | 12.19 | 20.17 | 32.96 | 13.29 |
| | HTVGNN | 17.38 | 28.53 | 11.47 | 18.18 | 29.86 | 11.93 | 19.41 | 31.68 | 12.74 |
| PEMS08 | HTVGNN-wc | 12.90 | 21.34 | 8.45 | 13.96 | 23.35 | 9.13 | 15.53 | 25.83 | 10.06 |
| | HTVGNN | 12.59 | 21.10 | 8.16 | 13.44 | 22.87 | 8.73 | 14.73 | 25.03 | 9.62 |

TABLE III. Validation of the effectiveness of coupled time-varying graphs in long-term prediction

significant benefits in reducing the cumulative prediction error. Detailed comparison results are presented in Table III.

The results presented in Table III unequivocally demonstrate the superiority of HTVGNN with coupling time-varying graphs over its counterpart without such coupling. This advantage becomes increasingly pronounced as the time step increases. Furthermore, Table 6 reveals that HTVGNN outperforms HTVGNN-wc by 3.92%, 4.04%, and 4.32% in terms of MAE, RMSE, and MAPE on PEMS04 dataset at a temporal resolution of 60 minutes, respectively. Similarly, on PEMS08 dataset at the same temporal resolution, HTVGNN achieves improvements of 5.43%, 3.20%, and 4.57% for MAE, RMSE, and MAPE.

G. Hyperparameters analysis of HTVGNN

We analyzed the time-varying graph embedding dimension represented by E, the model embedding dimension represented by D, the number of ETP multi-head self-attention heads represented by Heads, and the number of layers of the model represented by Layers. These four hyperparameters have significant effects on PEMS04 and PEMS08 data. The influence of the set of experimental results, the value of D on the data set PEMS04 is 4 to 10, and the value of D on the data set PEMS08 is 2 to 8.

- 1) Sensitivity to Layers: The impact of the model's layer count is illustrated in Fig. 5a. However, our findings indicate that increasing the number of layers does not yield a significant improvement in performance. This observation suggests that the HTVGNN model may have reached its predictive error limit.
- 2) Sensitivity to Heads: The impact of the number of heads on RTP multi-head attention is illustrated in Fig. 5b. It can be observed from the figure that while the attention score can be effectively computed with two heads, the dimensionality of the corresponding space for this head count is insufficient. As the number of heads increases, spatio-temporal information is mapped to a higher-dimensional space, resulting in more reasonable correlation coefficient scores. However, an excessively large number of heads may introduce numerous negative high-dimensional spaces, which hinders accurate calculation of the attention score.
- 3) Sensitivity to Dimensions: The impact of the hidden embedding dimension D is illustrated in Fig. 5c. As depicted, smaller dimensions fail to effectively encode spatiotemporal information, while excessively large ones may lead to overfitting.

4) Sensitivity to E: The impact of the size E in the embedding space for time-varying graphs is illustrated in Fig. 5d. From the figure, it can be observed that a smaller dimension E fails to capture spatial correlations effectively, while an excessively large dimension E leads to overfitting and suboptimal learning of time-varying graphs.

H. Visualiation

In order to visually demonstrate the superiority of our proposed model, we present results of various benchmark models at 500 time steps on PEMS04 and PEMS08 datasets. The comparison between traffic flow prediction results and actual values is depicted in Fig.7. It can be observed that the HTVGNN model exhibits enhanced accuracy and responsiveness towards abnormal traffic flow, while also demonstrating reduced error in handling complex and dynamic traffic patterns.

I. Efficiency Study

Additionally, we conducted a comparison of the training and inference efficiency of HTVGNN, Bi-STAT, and PDFormer on the PEMS04 dataset. To ensure fairness in our evaluation, all methods were executed on a server equipped with an Intel Core i7 13700KF processor and a single NVIDIA RTX graphics card. The results of this comparison are presented in Table 9.

As shown in Table 9, despite the time-consuming nature of RNNs, the HTVGNN model utilizes a single layer. In contrast, PDFormer and Bi-STAT solely rely on transformerbased architectures that inherently support parallel processing. However, to capture deep spatio-temporal correlations, transformer-based models often require multiple layers; for instance, PDFormer employs six layers while Bi-STAT uses two layers. Nevertheless, due to the inclusion of a recollection process, this model incurs twice the original time complexity. Consequently, these transformer-only models do not offer any advantage in terms of time complexity. Conversely, our proposed HTVGNN model achieves superior prediction error performance on PEMS04 dataset with just one layer despite employing computationally intensive RNNs. Moreover, HTVGNN significantly outperforms PDFormer and Bi-STAT in prediction accuracy while maintaining similar computational requirements.

VI. CONCLUSION

In this paper, we propose a novel hybrid time-varying graph neural network prediction method. To accurately capture

the most relevant temporal features in temporal correlation modeling, we introduce a time-aware multi-head attention mechanism based on time-varying mask enhancement. We allocate the optimal attention calculation scheme for different temporal features. In spatial correlation modeling, we employ two strategies. Firstly, in static spatial correlation modeling, we design a coupled graph learning mechanism to integrate the graph learned at each time step and effectively enhance the model's long-term prediction capability. Secondly, in dynamic spatial correlation modeling within the road network, we define a mask based on topological matrix and semantic matrix to optimize the dynamic time-varying graph and improve the model's ability to capture dynamic spatial correlations. Simulation experiments conducted on four real datasets validate our proposed method HTVGNN by demonstrating its superior prediction accuracy compared with state-of-the-art spatio-temporal graph neural network models. Furthermore, our proposed coupling graph learning method significantly improves long-term prediction performance of the model as observed in ablation experiments. Future work will focus on exploring more effective masking techniques through model pre-training and providing more efficient yet powerful masking mechanisms for Transformer models.

REFERENCES

- H. Yan, X. Ma, and Z. Pu, "Learning dynamic and hierarchical traffic spatiotemporal features with transformer," *IEEE Transactions on Intelligent Transportation Systems*, vol. 23, no. 11, pp. 22386–22399, 2021.
- [2] B. Pan, U. Demiryurek, and C. Shahabi, "Utilizing real-world transportation data for accurate traffic prediction," in 2012 ieee 12th international conference on data mining. IEEE, 2012, pp. 595–604.
- [3] Y. Sun, G. Zhang, H. Yin et al., "Passenger flow prediction of subway transfer stations based on nonparametric regression model," Discrete Dynamics in Nature and Society, vol. 2014, 2014.
- [4] B. M. Williams, "Multivariate vehicular traffic flow prediction: evaluation of arimax modeling," *Transportation Research Record*, vol. 1776, no. 1, pp. 194–200, 2001.
- [5] B. M. Williams, P. K. Durvasula, and D. E. Brown, "Urban freeway traffic flow prediction: application of seasonal autoregressive integrated moving average and exponential smoothing models," *Transportation Research Record*, vol. 1644, no. 1, pp. 132–141, 1998.
- [6] E. Zivot and J. Wang, "Vector autoregressive models for multivariate time series," *Modeling financial time series with S-PLUS®*, pp. 385– 429, 2006.
- [7] M. Awad, R. Khanna, M. Awad, and R. Khanna, "Support vector regression," Efficient learning machines: Theories, concepts, and applications for engineers and system designers, pp. 67–80, 2015.
- [8] J. Van Lint and C. Van Hinsbergen, "Short-term traffic and travel time prediction models," *Artificial Intelligence Applications to Critical Transportation Issues*, vol. 22, no. 1, pp. 22–41, 2012.
- [9] R. Fu, Z. Zhang, and L. Li, "Using 1stm and gru neural network methods for traffic flow prediction," in 2016 31st Youth academic annual conference of Chinese association of automation (YAC). IEEE, 2016, pp. 324–328.
- [10] Y.-S. Jeong, Y.-J. Byon, M. M. Castro-Neto, and S. M. Easa, "Supervised weighting-online learning algorithm for short-term traffic flow prediction," *IEEE Transactions on Intelligent Transportation Systems*, vol. 14, no. 4, pp. 1700–1707, 2013.
- [11] J. Bai, J. Zhu, Y. Song, L. Zhao, Z. Hou, R. Du, and H. Li, "A3t-gcn: Attention temporal graph convolutional network for traffic forecasting," ISPRS International Journal of Geo-Information, vol. 10, no. 7, p. 485, 2021.
- [12] K. Sun, Z. Zhu, and Z. Lin, "Adagen: Adaboosting graph convolutional networks into deep models," arXiv preprint arXiv:1908.05081, 2019.
- [13] Z. Wu, S. Pan, F. Chen, G. Long, C. Zhang, and S. Y. Philip, "A comprehensive survey on graph neural networks," *IEEE transactions on neural networks and learning systems*, vol. 32, no. 1, pp. 4–24, 2020.

- [14] B. Yu, H. Yin, and Z. Zhu, "Spatio-temporal graph convolutional networks: A deep learning framework for traffic forecasting," arXiv preprint arXiv:1709.04875, 2017.
- [15] M. Li and Z. Zhu, "Spatial-temporal fusion graph neural networks for traffic flow forecasting," in *Proceedings of the AAAI conference on artificial intelligence*, vol. 35, no. 5, 2021, pp. 4189–4196.
- [16] L. Bai, L. Yao, C. Li, X. Wang, and C. Wang, "Adaptive graph convolutional recurrent network for traffic forecasting," *Advances in neural information processing systems*, vol. 33, pp. 17804–17815, 2020.
- [17] P. Veličković, G. Cucurull, A. Casanova, A. Romero, P. Lio, and Y. Bengio, "Graph attention networks," arXiv preprint arXiv:1710.10903, 2017.
- [18] Y. Wang, X. Yu, S. Zhang, P. Zheng, J. Guo, L. Zhang, S. Hu, S. Cheng, and H. Wei, "Freeway traffic control in presence of capacity drop," *IEEE Transactions on Intelligent Transportation Systems*, vol. 22, no. 3, pp. 1497–1516, 2020.
- [19] E. Zivot and J. Wang, "Vector autoregressive models for multivariate time series," *Modeling financial time series with S-PLUS®*, pp. 385– 429, 2006.
- [20] I. Sutskever, O. Vinyals, and Q. V. Le, "Sequence to sequence learning with neural networks," Advances in neural information processing systems, vol. 27, 2014.
- [21] Y. Liu, H. Zheng, X. Feng, and Z. Chen, "Short-term traffic flow prediction with conv-lstm," in 2017 9th International Conference on Wireless Communications and Signal Processing (WCSP). IEEE, 2017, pp. 1–6.
- [22] Z. Wu, S. Pan, G. Long, J. Jiang, and C. Zhang, "Graph wavenet for deep spatial-temporal graph modeling," arXiv preprint arXiv:1906.00121, 2019
- [23] A. Dosovitskiy, L. Beyer, A. Kolesnikov, D. Weissenborn, X. Zhai, T. Unterthiner, M. Dehghani, M. Minderer, G. Heigold, S. Gelly et al., "An image is worth 16x16 words: Transformers for image recognition at scale," arXiv preprint arXiv:2010.11929, 2020.
- [24] J. Devlin, M.-W. Chang, K. Lee, and K. Toutanova, "Bert: Pre-training of deep bidirectional transformers for language understanding," arXiv preprint arXiv:1810.04805, 2018.
- [25] Z. Liu, Y. Lin, Y. Cao, H. Hu, Y. Wei, Z. Zhang, S. Lin, and B. Guo, "Swin transformer: Hierarchical vision transformer using shifted windows," in *Proceedings of the IEEE/CVF international conference on computer vision*, 2021, pp. 1012–10022.
- [26] H. Yan, X. Ma, and Z. Pu, "Learning dynamic and hierarchical traffic spatiotemporal features with transformer," *IEEE Transactions on Intelligent Transportation Systems*, vol. 23, no. 11, pp. 22386–22399, 2021.
- [27] X. Wang, Y. Ma, Y. Wang, W. Jin, X. Wang, J. Tang, C. Jia, and J. Yu, "Traffic flow prediction via spatial temporal graph neural network," in Proceedings of the web conference 2020, 2020, pp. 1082–1092.
- [28] B. Lu, X. Gan, H. Jin, L. Fu, and H. Zhang, "Spatiotemporal adaptive gated graph convolution network for urban traffic flow forecasting," in Proceedings of the 29th ACM International conference on information & knowledge management, 2020, pp. 1025–1034.
- [29] L. Bai, L. Yao, C. Li, X. Wang, and C. Wang, "Adaptive graph convolutional recurrent network for traffic forecasting," *Advances in neural information processing systems*, vol. 33, pp. 17804–17815, 2020.
- [30] W. Chen, L. Chen, Y. Xie, W. Cao, Y. Gao, and X. Feng, "Multi-range attentive bicomponent graph convolutional network for traffic forecasting," in *Proceedings of the AAAI conference on artificial intelligence*, vol. 34, no. 04, 2020, pp. 3529–3536.
- [31] J. D. Hamilton, Time series analysis. Princeton university press, 2020.
- [32] Y. Li, R. Yu, C. Shahabi, and Y. Liu, "Diffusion convolutional recurrent neural network: Data-driven traffic forecasting," arXiv preprint arXiv:1707.01926, 2017.
- [33] S. Guo, Y. Lin, N. Feng, C. Song, and H. Wan, "Attention based spatial-temporal graph convolutional networks for traffic flow forecasting," in *Proceedings of the AAAI conference on artificial intelligence*, vol. 33, no. 01, 2019, pp. 922–929.
- [34] C. Zheng, X. Fan, C. Wang, and J. Qi, "Gman: A graph multi-attention network for traffic prediction," in *Proceedings of the AAAI conference* on artificial intelligence, vol. 34, no. 01, 2020, pp. 1234–1241.
- [35] H. Yan, X. Ma, and Z. Pu, "Learning dynamic and hierarchical traffic spatiotemporal features with transformer," *IEEE Transactions on Intelligent Transportation Systems*, vol. 23, no. 11, pp. 22 386–22 399, 2021.
- [36] Y. Sun, X. Jiang, Y. Hu, F. Duan, K. Guo, B. Wang, J. Gao, and B. Yin, "Dual dynamic spatial-temporal graph convolution network for traffic prediction," *IEEE Transactions on Intelligent Transportation Systems*, vol. 23, no. 12, pp. 23 680–23 693, 2022.
- [37] J. Jiang, C. Han, W. X. Zhao, and J. Wang, "Pdformer: Propagation delay-aware dynamic long-range transformer for traffic flow prediction," arXiv preprint arXiv:2301.07945, 2023.

- [38] C. Chen, Y. Liu, L. Chen, and C. Zhang, "Bidirectional spatial-temporal adaptive transformer for urban traffic flow forecasting," *IEEE Transactions on Neural Networks and Learning Systems*, 2022.
- [39] C. Chen, K. Petty, A. Skabardonis, P. Varaiya, and Z. Jia, "Freeway performance measurement system: mining loop detector data," *Transportation Research Record*, vol. 1748, no. 1, pp. 96–102, 2001.
 [40] J. Liu, Y. Kang, H. Li, H. Wang, and X. Yang, "Stghtn: Spatial-temporal
- [40] J. Liu, Y. Kang, H. Li, H. Wang, and X. Yang, "Stghtn: Spatial-temporal gated hybrid transformer network for traffic flow forecasting," *Applied Intelligence*, vol. 53, no. 10, pp. 12472–12488, 2023.
- [41] Q. Ma, W. Sun, J. Gao, P. Ma, and M. Shi, "Spatio-temporal adaptive graph convolutional networks for traffic flow forecasting," *IET Intelligent Transport Systems*, vol. 17, no. 4, pp. 691–703, 2023.
- [42] Y. Bao, J. Huang, Q. Shen, Y. Cao, W. Ding, Z. Shi, and Q. Shi, "Spatial-temporal complex graph convolution network for traffic flow prediction," Engineering Applications of Artificial Intelligence, vol. 121, p. 106044, 2023.
- [43] I. Loshchilov and F. Hutter, "Decoupled weight decay regularization," arXiv preprint arXiv:1711.05101, 2017.